Catalysis Science & Technology

Accepted Manuscript

ROYAL SOCIETY OF CHEMISTRY

www.rsc.org/catalysis

Catalysis Science & Technology RSCPublishing

ARTICLE

Cite this: DOI: 10.1039/x0xx00000x

Metal-Free B-Doped Graphene with Efficient Electrocatalytic Activity for Hydrogen Evolution Reaction

Received 00th January 2012,
Accepted 00th January 2012

DOI: 10.1039/x0xx00000x

www.rsc.org/

Bhaskar R. Sathe,[a,b] Xiaoxin Zou,[a,b] and Tewodros Asefa[a,b]*

The chemical and physical properties of carbon nanomaterials such as graphene can be tailored by doping their structures with heteroatoms. However, substitutional doping of heteroatoms within carbon nanomaterials requires not only rational synthetic methods but also heteroatom-doping reagents that are easier to employ. Herein we report a facile, wet chemical synthetic method to metal-free, yet catalytically active, B-substituted graphene (B-SuG) by using BH_3-THF—a simple and commercially available borylation reagent. Moreover, we show that the B-doped material (*i.e.*, B-SuG) can serve as an efficient metal-free electrocatalyst for hydrogen evolution reaction (HER). Additionally, we demonstrate that BH_3-THF is a better borylating agent in terms of producing the most effective electrocatalyst than other borylating chemical agents such as $NaBH_4$, $B(OH)_3$, carborane, B_2O_3 and NH_3-BH_3, which we also tried under identical synthetic conditions. Compared with the conventional heteroatom-doping methods used for graphene, such as chemical vapor deposition (CVD) and physical vapor deposition (PVD), BH_3-THF certainly also has the added advantage of being more amenable and easier to use. We expect that the work will stimulate future research on synthesis of other innovative and sustainable metal-free materials and catalysts and investigation of fundamental structure-property relationships in metal-free catalysts/catalysis for renewable energy and other applications.

1. Introduction

In the face of declining non-sustainable energy resources such as petroleum and, more importantly, their unabated negative environmental impacts, H_2 has long been considered as one of the most promising sources of clean, renewable energy that can meet these challenging problems. However, to make H_2 economy a reality, efficient electrocatalysts and catalytic technologies that allow sustainable generation of molecular H_2 from water *via* catalytic hydrogen evolution reaction (HER) must be developed.[1-3] Although Pt and related noble metals are efficient electrocatalysts for this reaction, their high cost as well as low abundance in the Earth's crust has been limiting their widespread uses.[4] While HER electrocatalysts based on non-noble metal (*e.g.*, Ni, Fe, Co, and Mo) complexes and their alloys and heterostructures can address some of these issues,[5] such metallic systems have inherent tendency to undergo oxidation, leaching, and/or sintering, and can thereby lose their catalytic activity under conditions in which HER is often carried out.[5,6] Hence, there has been a burgeoning interest in the development of HER electrocatalysts that are completely metal-free and robust yet efficient and inexpensive.

The discovery of various types of advanced metal-free materials such as graphene, carbon nanotubes, and rubrene that possess not only interesting properties but also properties akin to those of metallic and semiconducing systems[7-9] has recently given way to research on the potential of such metal-free systems for various applications, including electrocatalysis. Graphene, in particular, has become highly attractive for electrocatalysis because of its superior chemical and thermal stability, excellent electronic and ionic conductivity, and tailorable and useful properties.[10-13] For example, by creating charged groups and defect sites on graphene through modification of the arrangements of its surface carbon atoms, defective graphene (DeG) materials with altered geometric and electronic structure and surface carbon atoms having low coordination numbers and/or free coordination sites can be produced.[14] When such materials are employed as electrocatalyst, they can render lower activation barriers or improved adsorption energy to reactants, products, or intermediate species, giving rise to higher catalytic activity and/or selectivity for certain electrocatalytic reactions.[14,15]

Besides defect sites, addition of reactive sites or heteroatoms (*e.g.*, B atoms or others) as dopant into graphene can modulate graphene's physical and chemical properties.[16-19] More importantly, this process can produce graphene-based materials without substantially compromised conductive properties, but with improved ability to adsorb the atomic/molecular species undergoing catalytic reactions. This is particularly well-demonstrated by using boron as dopant.[20-23] However, despite intensive theoretical and experimental studies of the properties of B-doped graphene materials, mainly for electronic and, to some extent, catalysis applications,[16-23] the synthesis of such materials remains challenging. As shown in a recent report, for example, thermal annealing of B-containing polycyclic aromatic hydrocarbons produces B-doped graphene clusters that are physically mixed with graphene (or that are not pure).[20] In another study, B-doped graphene containing some oxygen atoms, for supercapacitor applications, was shown to form inadvertently when borane was used as a reductant to reduce graphene oxide into graphene.[22,24] Otherwise, the major synthetic methods reported to date for making B-doped graphene remain chemical vapor deposition (CVD) and physical vapour deposition (PVD),[16] techniques that are relatively more costly to apply and often produce only a small amount of the desired material.

Herein we report a facile wet chemical synthetic method to electrocatalytically active, B-substituted graphene (B-SuG). The material is synthesised by controlled substitution of the C atoms of defective graphene (DeG) with B atoms using a simple and commercially available borylating agent borane.tetrahydrofuran (BH_3-THF) (Scheme 1). We also demonstrate that the resulting material (*i.e.*, B-SuG) can serve as an efficient metal-free electrocatalyst for HER. Moreover, we show that BH_3-THF is much better borylation reagent to yield efficient B-doped electrocatalyst for HER, compared with many other borylation reagents such as $NaBH_4$, $B(OH)_3$, carborane, B_2O_3, and NH_3-BH_3. It is also worth noting that, to the best of our knowledge, this is the first time that a B-doped graphene material is shown to have electrocatalytic activity toward HER.

2. Experimental section

2.1. Reagents and materials

Graphite (45 μm, >99.99 wt. %), BH_3-THF, hydrochloric acid (37.5 %), sulphuric acid (96 %), and nitric acid (70.4 %) were all purchased from Sigma-Aldrich. Tetrahydrofuran (THF) and absolute ethanol (99.99%) were obtained from Fischer Scientific. All the chemical reagents were of analytical grade and used as received without further purification. Deionized water was used as a solvent throughout the synthesis of the materials as well as for studies of their electrochemical and electrocatalytic properties.

2.2. Oxidative exfoliation of graphite to graphene oxide (GO)

Graphene oxide (GO) was prepared *via* exfoliation of graphite powder using the Hummer's method[S1] with slight modification. In a typical synthesis, 1 g of graphite powder was mixed with an acidic solution containing 45 mL of concentrated nitric acid and 90 mL of sulfuric acid in a round-bottomed flask, and the mixture was stirred in ice-bath for 30 min. The ice bath was then removed, and the dispersion in the round-bottomed flask was sonicated over an ultra-sonicator (Branson 2510, USA) at room temperature for 2 h. The dispersion was subsequently refluxed for 24 h, during which time the reaction progressed, gradually forming a brown-grey paste with diminished effervescence. After separating it via centrifugation, the brown-grey paste was re-dispersed in deionized (DI) water with sonication for 3 h. The dispersion was filtered and the solid material

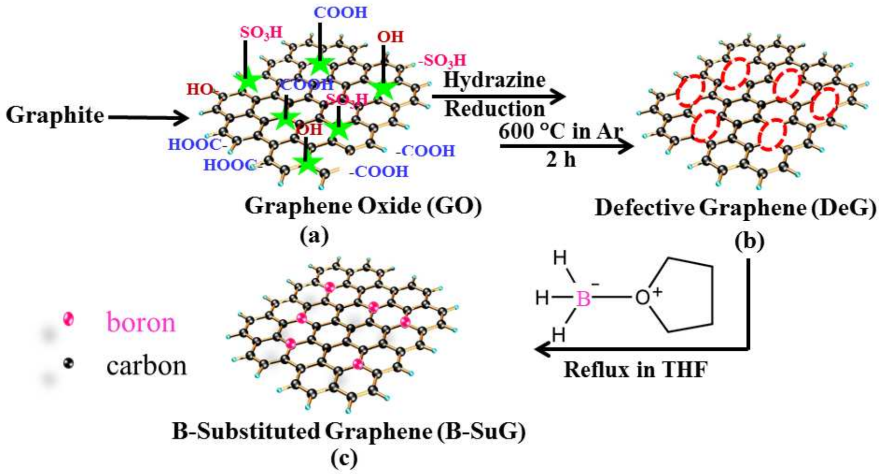

Scheme 1. Schematic representation of the various steps employed for the synthesis of B-substituted graphene (B-SuG): (a) oxidative exfoliation of graphite to graphene oxide (GO), (b) chemical reduction, followed by thermal treatment, of GO to form defective graphene (DeG), and (c) finally, borylation of DeG with BH_3-THF to dope the defective sites of DeG with B atoms and produce the desired material, B-SuG.

Catalysis Science & Technology RSCPublishing

ARTICLE

was washed with 1 M HCl, followed by copious amount of DI water until the hydrated gel turned into a black powdered material. The black powdered material (graphite oxide) was dispersed in anhydrous THF and sonicated for 1 h to exfoliate the graphite oxide into GO sheets. The solution containing GO was then separated from the residual unreacted graphite, which quickly precipitated out in the THF solution. The solid product was recovered from the solution via centrifugation of the dispersion and then dried under high vacuum at 40 °C, yielding GO in powdered form. The GO was dispersed in DI water, giving a brownish suspension that remained stable for over 2 weeks. The GO was then converted to defective graphene (DeG) and B-substituted graphene (B-SuG) in subsequent steps.

2.3. Synthesis of Defective Graphene (DeG)

In a typical synthetic procedure, GO (100 mg) taken from the stock solution above was mixed with water (100 mL) in a 250-mL round-bottomed flask. The resulting yellow-brown dispersion was sonicated with an ultrasonicator until the solution became clear. After adding hydrazine hydrate (1.00 mL) into it, the dispersion was heated in an oil bath at 100 °C for 24 h. During this time, a black solid product (*i.e.*, reduced GO) began to form and gradually precipitate out. The reduced GO was isolated by centrifugation and washed copiously with water and ethanol to remove the residual hydrazine hydrate and any other side products from it. After drying under ambient conditions, the resulting chemically reduced GO was further treated at 700 ºC under constant flow of N_2 gas for 6 h to further remove any remaining organic functional groups present on it. This finally yielded defective graphene, denoted here as DeG.

2.4. Synthesis of B-Substituted Graphene (B-SuG)

DeG (100 mg) was mixed with THF (100 mL) in a 250 mL round-bottomed flask. The resulting yellow-brown dispersion was sonicated until it became clear. After adding a calculated amount of BH_3-THF (1.2 mL) in it, the dispersion was heated under mild stirring in an oil bath at 80 °C for 24 h. This led to the gradual formation of a black precipitate. The solid product was isolated by centrifugation and washed copiously with THF and then ethanol to remove unreacted BH_3-THF or other impurities from it. After drying the solid product under ambient conditions, followed by under high vacuum at 40 ºC for 6 h, the desired product (B-SuG) was obtained. By following the same procedure but using other borylating agents, namely $NaBH_4$, $B(OH)_3$, carborane, and B_2O_3, other boron-doped graphene materials / electrocatalysts, which were used as reference materials for comparative studies, were also synthesized.

2.5. Instrumentations for structural and compositional characterization

The structures and composition of the materials were characterized using the following instrumentations. Transmission electron microscope (TEM) images were obtained using a Topcon 002B TEM microscope operating at 200 kV. X-ray photoelectron spectroscopy (XPS) was performed using a Thermo K-Alpha XPS system (Thermo Scientific, USA) equipped with an Al Kα radiation source with a 400 μm spot size. During the XPS experiments, an electron flood gun was used to minimize charging while an energy resolution of 1 eV was employed for the survey scans and an energy resolution of 0.1 eV was used for the high resolution scans of individual peaks. The system's vacuum level was brought to $< 10^{-8}$ Torr during the data collection. Raman spectroscopy was performed on a Renishaw inVia Raman microscope, equipped with a 532 nm He-Ne laser. A typical laser power of 2.0 mW and an exposure time of 10 s were used at the sample position during the experiments.

2.6. Electrocatalytic activity measurements

All the electrochemical measurements were performed with a PAR Versastat3 (Princeton Applied Research, PAR) potentiostat using a standard three electrode cell at room temperature. The cell consisted of a working electrode, a counter electrode, and a reference electrode that are comprised of a glassy carbon electrode (GCE; 3 mm in diameter, from ECO CHEMIE) disc modified with either the B-SuG or the control samples, a carbon rod, and a saturated calomel electrode (SCE), respectively. Before each experiment, the GCE was polished with 0.05 mm alumina slurry and then sonicated in DI water for 10 min. The working electrode was prepared by drop-casting on the GCE a 10 μL aliquot of the slurry, which was made by sonicating a calculated amount of the graphene-based electrocatalysts or the other control samples in 1 mL isopropyl alcohol. Then, 2 μL of 0.01 wt. % Nafion in ethanol was casted on the electrocatalyst layer, forming a uniform thin film. The electrode was then dried in air before being used in the electrochemical cell.

Rotating disc electrode (RDE) based studies to probe the kinetics of the electrocatalytic reactions were performed by preparing the samples in the same way. This experiment was performed using an Autolab PGSTAT30 (Eco Chemie) potentiostat, again with a conventional three-electrode test cell consisting of a 0.07065 cm^2 GCE coated with the samples as the working electrode, Pt as the quasi-reference electrode, and Pt foil as the counter electrode. The measurements were done at a scan rate of 10 mV/s and at various rotating speeds, *i.e.*, 400, 900, 1200, 1600, and 2500 rpm.

3. Results and discussion

3.1. Synthesis and characterization

The synthesis of B-SuG involved three steps: the preparation of graphene oxide (GO),[25] the conversion of GO to DeG, and finally the treatment of DeG with BH_3-THF to form B-SuG (see Scheme 1 and the Experimental Section above for details). In the first step, graphite was converted to GO by treating the former with concentrated nitric acid/sulfuric acid solution. In the process, some of the graphite's sp^2 carbon atoms were transformed into sp^3 carbon atoms as the graphite underwent oxidation and its basal (and edge) plane carbons were functionalized with -COOH, -SO_3H, -OH and epoxy groups by the strong acid solution.[26] Additionally, after such chemical treatment (*i.e.*, graphite with such strong acids), the resulting material (GO) is well-known to have ill-defined distribution of C atoms or some defect sites and high degree of structural disorder on its basal planes.[14,24] Thus, the as-obtained GO was chemically reduced and converted into DeG in order to partially restore the material's sp^2 C platform, and thereby its conductivity, so that it will be suitable for making electrocatalyst with. More importantly, this chemical reduction step was performed in order to create some open sites on the basal planes of the material so that it can readily undergo B-doping. Accordingly, upon treatment with BH_3-THF at 80 ºC, the open sites of DeG, which are surrounded by sp^2-hybridized C atoms, were filled in with B atoms, and the desired B-SuG material was obtained.

The superimposed X-ray diffraction (XRD) patterns of DeG and B-SuG are displayed in Fig. 1a. The XRD patterns show that both samples have Bragg reflections corresponding to the (002), (101), (110) and (201) planes of graphene.[27] However, some subtle differences are also evident in the crystallographic structure of the materials, specifically suggesting a slight increase in the interlayer spacing of B-SuG compared with that of DeG. This is especially true upon comparing the (002) diffraction line of B-SuG with that of DeG (inset in Fig. 1a); this difference in the XRD patterns of the two materials is presumably caused by the substitution of the C atoms of DeG with B atoms. Additional inspection of the XRD patterns reveals that there is(are) no new diffraction peak(s) associated with pure boron and/or other boron-based species, such as $(BN)_x$, borates, $(CB)_x$, etc., in the B-SuG material. This also indicates that the boron species in B-SuG are most likely present only as chemically substituted moieties within the electron-rich defective C structures, rather than in form of some clusters. This is supported by TEM images, which showed barely any difference between the structures of DeG and B-SuG, or more importantly, gave no indication of formation of B-based clusters or nanoparticles in B-SuG (Figs. 1b and S1).

X-ray photoelectron spectroscopy (XPS) was used to probe the composition of the materials as well as the nature of the B atoms in the B-SuG material. The full range survey XPS spectra depicting the B1s, C1s and O1s peaks of B-SuG and the core level peaks of C1s and O1s of DeG are provided in Figs. S2 and S3. The result in Fig. S3, in particular, clearly shows the

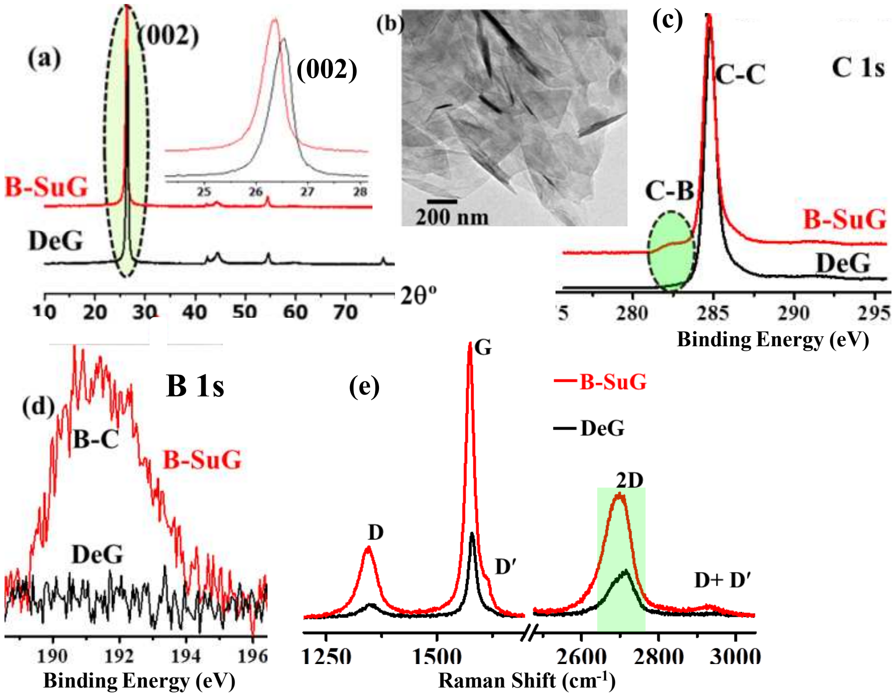

Figure 1. (a) Superimposed X-ray diffraction (XRD) patterns of DeG and B-SuG, (b) TEM image of B-SuG, (c) C1s and (d) B1s XPS spectra of DeG and B-SuG, and (e) superimposed Raman spectra of DeG and B-SuG. The intensity ratios of the various Raman peaks observed in the spectra are compiled in Table 1.

Table 1. Raman spectroscopic and electrical conductivity (Z_f) data for DeG and B-SuG, which was obtained by chemical doping using BH_3-THFas the source of boron.

Sample	Raman Shift (cm^{-1})					I_G/I_D	I_{2D}/I_G	Z_f (Ω)
	D	G	D′	2D	D + D′			
DeG	1350	1583	--	2710	--	4.93	0.57	2300
B-SuG	1350	1579	1620	2700	2930	3.69	0.46	299

presence of B, C and O atoms in the B-SuG, with atomic percentage of 1.85 %, 88.96 % and 5.45 %, respectively. This is fairly similar to the results obtained with elemental analysis: i.e., 1.01, 92.90, and 5.99 at. %, respectively. Figs 1c and 1d display the superimposed XPS spectra of core-level C1s and B1s electrons, respectively, of the DeG and B-SuG samples. The C1s spectrum of B-SuG shows two signals at binding energy (BE) of ~282.4 and ~284.7 eV, which correspond to the C atoms in C-B and sp^2-hybridized C-C moieties, respectively.[28] The down-shift in BE of B-SuG can be attributed to the decrease in the Fermi level of this material as a result of formation of chemical bonds between its C atoms and the electron-deficient B dopants in it. Besides having lower BE, the C1s peak associated with the C atoms of C-B in B-SuG showed a slightly higher full width at half maximum (FWHM) compared with that of the latter. The higher FWHM in B-SuG can be attributed to the presence of increased structural disorder by virtue of the formation of heteroatomic (C-B) bond in it, as evidenced by FT-Raman spectroscopic analyses (see below). The presence of substitutional B atoms or C-B species in the structure of B-SuG is further verified by analyzing the B1s peak in the XPS spectrum (Fig. 1d). In particular, the strong peak observed at ~189.85 eV is a clear indication of the presence of C-B species[29] in B-SuG, which is possible only from the substitution of C atoms of graphene by the B atoms from BH_3-THF. This result is also in line with previous reports, in which the BEs of the B atoms bonded to B, C, O and N atoms were documented to be in the range of ~188-198 eV and their values were reported to increase in the order of B-B < B-C < B-O ≈ B-N.[30-31]

Next, we employed Raman spectroscopy to further probe the B-doped graphene by BH_3-THF. The superimposed Raman spectra of B-SuG and its precursor (DeG) are shown in Figure 1e, and their representative major bands are summarized in Table 1. The results indicate that B-SuG exhibits an intense D band, which is caused by the formation of significant defect or disordered sites in its structure. The spectra also show a G band corresponding to crystalline graphitic structure, along with a wide 2D band (a second-order phonon mode) that indicates the existence of a substantial defect in the structure of B-SuG.

By analyzing the intensity of its defect-induced Raman peaks (*i.e.*, D, 2D, and D′) with respect to that of its G band, the nature and extent of defect sites and chemical disorder in graphene can be determined.[32] Accordingly, we used the data from the Raman spectra, specifically the I_G/I_D ratio, to obtain the degree of defect in B-SuG *vis-à-vis* with its parent materials (Table 1). The I_G/I_D ratio for B-SuG is found to be ~3.69, which is lower than that of DeG (~4.93); this indicates that more defects are present in the former, presumably due to the presence of substitutional B atoms in its network. Remarkably, besides the difference in shape/symmetry of their G-bands, the major difference between the Raman spectra of B-SuG and DeG is the presence of more intense D band at ~1350 cm^{-1} and the appearance of D′ band at ~1620 cm^{-1} in the former. This further supports our conclusion that B atoms were successfully doped within DeG after treatment of the latter with BH_3-THF. The result is also in good agreement with the Raman spectra data reported for B-doped graphene synthesized by mechanical exfoliation, which also showed more intense signals corresponding to the defect-induced D, D′ and 2D bands compared with those of pristine graphene.[33]

The Raman spectra data further reveals that the value of I_{2D}/I_G for B-SuG is smaller than the corresponding value for DeG (Table 1). The fact that the I_{2D}/I_G for B-SuG is lower than the corresponding value for DeG can be attributed to the increase in absolute value of the Fermi level[34] in the former. This is verified by electrical conductivity and electrochemical impedance spectral (EIS) studies of the two materials and comparing their Faradic impedance values (Z_f) (Table 1). The results indicate that B-SuG exhibits a much lower resistance to charge-transfer (~229 Ω) than does DeG (~2.3 kΩ). The significantly reduced resistance to charge-transfer in B-SuG implies that this material gives a markedly faster electron transfer pathway at its interface during electrochemical processes. This is actually to be expected as the introduction of B atoms in graphene can create additional holes within the valence band of the material, increasing the carrier concentration and density of states (DOS) at the electrified interface of B-SuG (compared with its parent material, DeG).[34] In other words, the increase in Fermi level of B-SuG can be attributed to the presence of B atoms in its structure.

Besides rendering a more intense G-band, the introduction of B atoms into DeG leads to a slight shift in some of the Raman bands. For instance, the 2D band of B-SuG red-shifts by ~15 cm^{-1} compared with the corresponding Raman band of DeG. This decrease in the vibrational frequency of 2D band is most likely due to the increase of the lattice constant of the material after B doping, as confirmed by XRD (Fig. 1a). In other words, these changes in band positions as well as intensities in the Raman bands all point to fact that B-SuG possesses more defect sites than its parent material (DeG). The results also confirm that changes in bond network and electronic structure occur in DeG upon B-doping.[35]

3.2. Electrocatalysis

Next, the electrocatalytic activities of the as-synthesized DeG and B-SuG for HER were evaluated and compared with each other as well as with those of other systems (see details in Supporting Information). The linear sweep voltammetry (LSV) experiment of B-SuG in HER in 0.5 M H_2SO_4 solution (Fig. 2a) shows an increase in current density at overpotential of as low as ~0.2 V vs RHE, beyond which the current density increases exponentially towards a more negative potential. In sharp contrast to this, DeG displays a relatively lower electrocatalytic activity towards HER as it does not give a good current density until it is at onset potential of ~0.3 V vs RHE. Nevertheless, both B-SuG and DeG show better electrocatalytic activity compared with a blank GC, graphite or GO. The considerably higher catalytic activity exhibited by B-SuG toward HER compared with DeG can only be attributed to the presence B atoms as dopant in B-SuG. This, in turn, can be correlated with the presence of surface defect sites and large number of surface active (electron rich) reduction centers due to the presence of B heteroatoms (C-B bonds) in the former, which can lead to lower conversion barriers for the transformation of H^+ ions to H_2.

By fitting the linear portions of the Tafel plots[36] (inset in Fig. 2a) to the Tafel equation (η = blog j + a, where j is the current density and b is the Tafel slope), Tafel slopes of ~99 and ~130 mV/decade and current densities of 14 x 10^{-4} mA/cm^2 and 1 x 10^{-4} mA/cm^2 for B-SuG and DeG, respectively, were obtained. These polarization studies and results clearly indicate that B-SuG can serve as an effective HER catalyst. For further evaluation of the electrochemical and electrocatalytic properties of the materials, impedance measurement at overpotential of η = 0.201 V vs RHE was conducted, and the results are presented in Fig 2b. The result reveals that B-SuG exhibits much lower

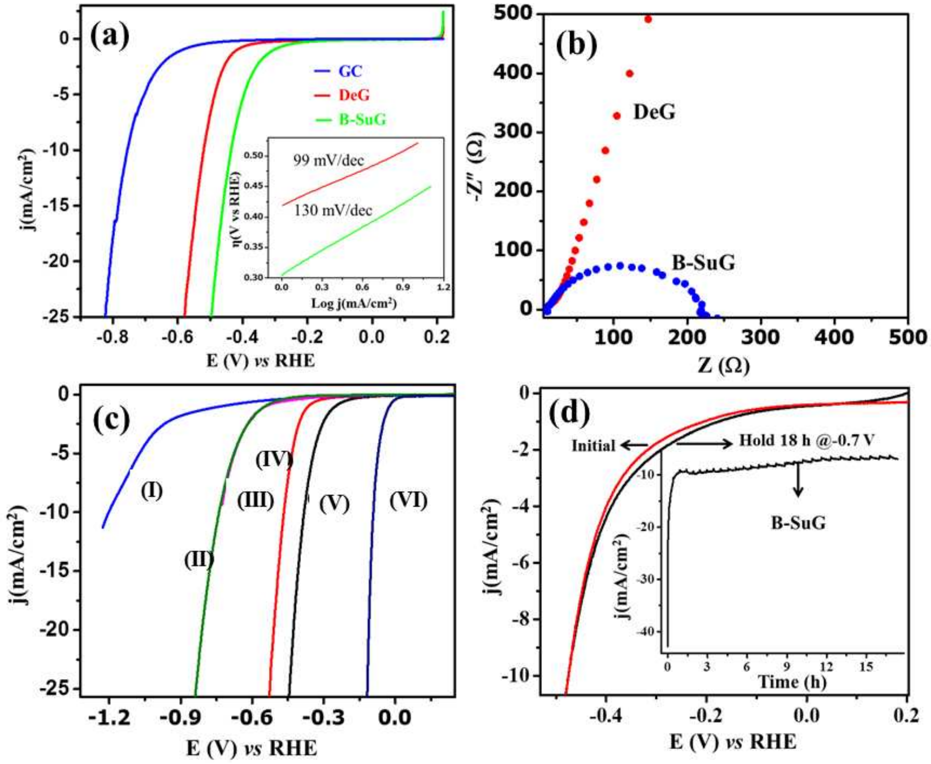

Figure 2. (a) Superimposed linear sweep voltammetry (LSV) curves of B-SuG, DeG, and a blank GC electrode, with their corresponding Tafel plots shown in inset. (b) Electrochemical impedance spectra (EIS) of DeG and B-SuG at an overpotential of 0.201 V vs RHE (c) Superimposed LSV curves of the various B-doped graphene materials that were synthesized under identical synthetic conditions but by using different borylating agents: I - carborane, II - $B(OH)_3$, III - $NaBH_4$, IV - DeG, and V - BH_3-THF (i.e., B-SuG). For comparison, the LSV curve of Pt is also included in VI. (d) Superimposed LSV recorded for B-SuG at initial measurement (red line) and after 18 h of j-t measurement (black line) at an applied potential of -0.7V vs RHE. The inset shows potentiostatic HER for B-SuG at -0.7 V vs RHE. The measurements were done at a sweep rate of 50 mV/s by using a scanning calomel electrode (SCE) as a reference electrode and a carbon rod as a counter-electrode in the potential range of 0 to -1 V vs RHE. Please note that the spikes seen on the current profile are due to the formation of H_2 bubbles on the planar disk electrode, an event that is common in such experiments.

impedance (Z_f) (*i.e.*, Faradaic or charge-transfer impedance) (≈ 229 Ω) than DeG (Z_f ≈ 2300 Ω). The significantly reduced Z_f for B-SuG suggests that graphene shows a markedly faster HER kinetics in electrocatalysis after B atoms are doped in it; this is possibly due to the synergistic roles that B atoms play at interface between the material and the electrode. This argument is made based on some earlier reports that showed synergistic effects and better electrocatalytic activity for other graphene-based hybrid systems. For Example, Dai *et al.* indicated that synergistic effects in MoS_2/reduced graphene oxide hybrid sheets could account for the better electrochemical and electrocatalytic activity, or the lower overpotential and Tafel slopes, exhibited by the hybrid material in HER compared with its constituents (*i.e.*, free MoS_2 flakes or reduced GO).[37]

The electrocatalytic activity of B-SuG was further evaluated by comparing its activity toward HER with those of the other B-modified graphene materials we synthesized with identical synthetic procedure but using other borylating agents, namely $NaBH_4$, $B(OH)_3$ and carborane (Fig. 2c). The results indicated that B-SuG showed better activity than all the other materials. This is most likely due to the fact that the latter materials all do have either O atoms or boron clusters in form of B-O or B-B units within their graphitic skeleton, as also indicated by others[22] (please note that such B-O or B-B species are not observed in the case of B-SuG, based on the XPS results and XPS peaks associated with these elements).

Finally, we performed i-t measurements for longer times (18 h) to assess the stability of B-SuG in HER. At the end of 18 h of i-t measurement, the reaction gave similar LSV curve as the one ran initially (Fig. 2d), with only negligible loss of the cathodic current (see inset in Fig. 2d); this clearly indicates that B-SuG is quite stable as electrocatalyst in HER.

As rotating disc electrode (RDE) studies allow accurate measurement of Ohmic and transport overpotentials, the results can provide reliable estimates of the intrinsic electrocatalytic activities of materials. Accordingly, the actual HER activities of the B-SuG catalyst and its control sample are probed using RDE based experiments. The results, which are compiled in Figure 3, show LSV curves recorded using catalyst-modified RDE rotating at different speeds in the rage of 0-2500 rpm for HER in 0.5 M H_2SO_4 at room temperature. The results indicate that the limiting current density is progressively increased with the RDE's rotation rate. Apart from this, the rate of increase in current density with rotation is higher in case of B-SuG (Figure 3b) compared with DeG (Figure 3a). These results indicate that the HER activity of B-SuG is higher than that of DeG, which is in good agreement with the results compiled in Figure 2 above.

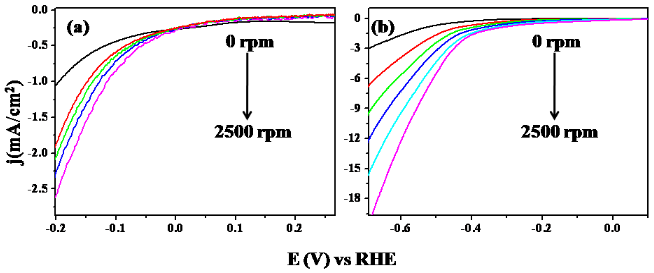

Figure 3. Superimposed linear sweep voltammetry (LSV) curves at a scan rate of 10 mV/s and at different rotation speeds in the range of 0 rpm-2500 rpm for the HER using (a) DeG and (b) B-SuG as electrocatalyst in 0.5 M H_2SO_4 at 298 K.

Conclusions

We described a facile, solution-based synthetic method to metal-free, B-substituted graphene (B-SuG) that is proven to be effective electrocatalyst for HER. The synthesis of the materials is achieved by borylation of defective graphene (DeG) using BH_3-THF, a simple and commercially available borylating agent. Moreover, we show that the B-SuG can efficiently serve as a metal-free electrocatalyst for hydrogen evolution reaction (HER) with better activity than other related materials prepared using other borylation chemical reagents, including $NaBH_4$, $B(OH)_3$, carborane, B_2O_3 and NH_3-BH_3. The synthetic approach can pave the way for future design and synthesis of other innovative and more sustainable metal-free materials and catalysts for renewable energy and other applications.

Acknowledgements

TA acknowledges the financial support of the US National Science Foundation (NSF) (Grant Nos.: NSF DMR-0968937 and NSF NanoEHS-1134289). BRS thanks the USIEF for the Fulbright-Nehru Postdoctoral Research Fellowships. We thank Mr. Vishal Dhavale at the National Chemical Laboratory, Pune, India, for his assistance with the RDE-based electrochemical measurements.

Notes and references

[a] *Department of Chemistry and Chemical Biology, Rutgers, The State University of New Jersey, 610 Taylor Road, Piscataway, NJ 08854, USA. E-mail: tasefa@rci.rutgers.edu*

[b] *Department of Chemical and Biochemical Engineering, Rutgers, The State University of New Jersey, 98 Brett Road, Piscataway, New Jersey 08854, USA.*

[c] *Institute for Advanced Materials, Devices and Nanotechnology, Rutgers, The State University of New Jersey, 607 Taylor Road, Piscataway, New Jersey 08854, USA.*

Electronic Supplementary Information (ESI) available: [details of any supplementary information available should be included here]. See DOI: 10.1039/b000000x/

1. (a) Xiang, Q. J.; Yu, J. G.; Jaroniec, M. *Nanoscale* 2011, **3**, 3670; (b) Y. Yu, J. Zhang, X. Wu, W. Zhao, B. Zhang, *Angew Chem. Int. Ed.*, 2012, **51**, 897.
2. H. Vrubel, T. Moehl, M. Grätzel, X. Hu, *Chem. Commun.*, 2013, **49**, 8985.
3. J. Tollefson, *Nature*, 2013, **464**, 1262.
4. R. Subbaraman, D. Tripkovic, D. Strmcnik, K. Chang, M. Uchimura, A. P. Paulikas, V. Stamenkovic, N. M. Markovic, *Science*, 2011, 1256.
5. V. S. Thoi, Y. Sun, J. R. Long, C. J. Chang, *Chem. Soc. Rev.*, 2013, **42**, 2388.
6. J. Greeley, T. F. Jaramillo, J. Bonde, I. B. Chorkendorff, J. K. Norskov, *Nat. Mater.*, 2006, **5**, 909.
7. (a) Q. Xiang, J. Yu, M. Jaroniec, *Chem. Soc. Rev*., 2012, **41**, 782; (b) Q. Xiang, J. Yu, M. Jaroniec, *J. Am. Chem. Soc.*, 2012, **134**, 6575.
8. B. R. Sathe, *RSC Adv.*, 2013, **3**, 5361.
9. (a) C. Zhu, S. Dong, *Nanoscale*, 2013, **5**, 1753; (b) D. Chen, L. Tang, J. Li, *Chem. Soc. Rev.*, 2010, **39**, 3157; (c) S. N. Kim, J. F. Rusling, F. Papadimitrakopoulos, *Adv. Mater.*, 2007, **19**, 3214.
10. X. Zhang, J. Xin, F. Ding, *Nanoscale*, 2013, **5**, 2556.
11. H. Bai, C. Li, G. Shi, *Adv. Mater.*, 2011, **23**, 1089.
12. C. Lee, X. Wei, J. W. Kysar, J. Hone, *Science*, 2008, **321**, 385.
13. (a) H. Zhang, K. Feng, B. Chen, Q. Meng, Z. Li, C. Tung, L. Wu *Catal. Sci. Technol.,* 2013, **3**, 1815; (b) N. G. Sahoo, Y. Pan, L. Li, S. H. Chan, *Adv. Mater.*, 2012, **24**, 4203. (c) Q. Xiang, J. Yu, *J. Phys. Chem. Lett.*, 2013, **4**, 753.
14. Q. Tang, Z. Zhou, Z. Chen, *Nanoscale*, 2013,**5**, 4541.
15. W. Tu, Y. Zhou, Z. Zou, *Adv. Funct. Mater.*, 2013, **23**, 4996.
16. L. Song, Z. Liu, A. L. M. Reddy, N. T. Narayanan, J. Taha-Tijerina, G. Peng, J. Lou, R. Vajtai, P. Ajayan, *Adv. Mater.*, 2012, **24**, 4878.
17. L. Qu, Y. Liu, J. B. Baek, L. Dai, *ACS Nano,* 2010, **4**, 1321.
18. S. Yang, L. Zhi, K. Tang, X. Feng, J. Maier, K. Mullen, *Adv. Funct. Mater.*, 2012, **22**, 3634.
19. Z.-S. Wu, A. Winter, L. Chen, Y. Sun, A. Turchanin, X. Feng, K. Mullen, *Adv. Mater.*, 2012, **24**, 5130.
20. Z. Jin, Z. Sun, L. J. Simpson, K. J. O. Neill, P. A. Parilla, Y. Li, N. P. Stadie,C. C. Ahn, C. Kittrell, J. M. Tour, *J. Am. Chem. Soc.*, 2010, **132**, 15246.
21. C. Dou, S. Saito, K. Matsuo, I. Hisaki, S. Yamaguchi, *Angew. Chem. Int. Ed.*, 2012, **51**, 12206.
22. J. Han, L. Zhang, S. Lee, J. Oh, K. Lee, J. R. Potts, J. Ji, X. Zhao, R. S. Ruoff, S. Park, *ACS Nano*, 2013, **7**, 19.
23. Y. Zheng, Y. Jiao, L. Ge, M. Jaroniec, S. Z. Qiao, *Angew. Chem. Int. Ed.*, 2013, **52**, 3110.
24. A. Staubitz, A. P. M. Robertson, M. E. Sloan, I. Manners, *Chem. Rev.*, 2010, **110**, 4023.
25. W. Hummers, R. Offeman, *J. Am. Chem. Soc.*, 1958, **80**, 1339.
26. B. R. Sathe, B. A. Kakade, A. Kushwaha, M. Aslam, V. K. Pillai, *Chem. Commun.*, 2010, **46**, 5671.
27. Z. H. Sheng, L. Shao, J. J. Chen, W. J. Bao, F. B. Wang, X. H. Xia, *ACS Nano*, 2011, **5**, 4350.
28. L. S. Panchalkarla, A. Govindraj, C. N. R. Rao, *ACS Nano*, 2007, **1**, 494.
29. L. S. Panchakarla, K. S. Subrahmanyam, S. K. Saha, A. Govindaraj, H. R. Krishnamurthy, U. V. Waghmare, C. N. R. Rao, *Adv. Mater.*, 2009, **21**, 4726.
30. Z. Wu, W. Ren, L. Xu, F. Li, H. Cheng, *ACS Nano*, 2011, **7,** 5463.
31. http://srdata.nist.gov/xps/
32. A. Eckmann, A. Felten, A. Mishchenko, L. Britnell, R. Krupke, K. S. Novoselov, C. Casiraghi, *Nano Lett.*, 2012, **12**, 3925.
33. Y. Kim, K. Fujisawa, H. Muramatsu, T. Hayashi, M. Endo, T. Fujimori, K. Kaneko, M. Terrones, J. Behrends, A. Eckmann, C. Casiraghi, K. Novoselov, R. Saito, M. Dresselhaus, *ACS Nano*, 2012, **6**, 6293.
34. A. Das, S. Pisana,B. Chakraborty, S. Piscanec, S. K. Saha, U. V. Waghmare, K. S. Novoselov, H. R. Krishnamurthy, A. K. Geim, A. C. Ferrari, A. K. Sood, *Nat. Nanotechnol.*, 2008, **3**, 210.
35. Q. H. Yang, P. X. Hou, M. Unno, S. Yamauchi, R. Saito, T. Kyotani, *Nano Lett.*, 2005, **5**, 2465.
36. C. R. Cox, M. T. Winkler, J. J. H. Pijpers, T. Buonassisi, D. G. Nocera, *Energy Environ. Sci.*, 2013, **6**, 532.
37. Y. Li, H. Wang, L. Xie, Y. Liang, G. Hong, H. Dai, *J. Am. Chem. Soc.*, 2011, **133**, 7296.
38. T. Hatakeyama, S. Hashimoto, S. Seki, M. Nakamura, *J. Am. Chem. Soc.*, 2011, **133**, 18614.

Table of Content Abstract and Graphic:

Metal-Free B-Substituted Graphene with an Enhanced Electrocatalytic Activity for Hydrogen Evolution Reaction

Bhaskar R. Sathe, Xiaoxin Zou, and Tewodros Asefa*

Graphical Abstract. We report a facile and inexpensive wet synthetic method to electrocatalytically active, B-substituted graphene (B-SuG) by controlled substitution of the C atoms of graphene with B atoms using BH_3-THF. The resulting material is shown to serve as an efficient metal-free electrocatalyst for hydrogen evolution reaction (HER). The synthetic approach can also pave the way for future design and synthesis of other innovative and more sustainable metal-free materials and catalysts for renewable energy and other applications.

Table of Content Graphic:

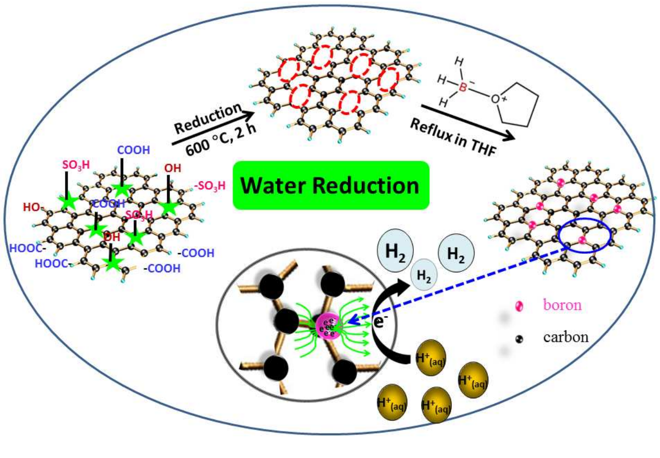

Keyword: Graphene, Water Reduction, Boron-Substituted Graphene, Electrocatalysis, Hydrogen Evolution Reaction, HER